

Green-Synthesis, Characterization and the Biological Evolution of ZnSnO₃

Y.V. BHASKARALAKSHMI^{1,*}, P. SWAPNA¹, B. KISHORE BABU² and Y. SRINIVASA RAO¹

¹Department of Instrument Technology, AU College of Engineering, Visakhapatnam-530003, India

²Department of Engineering Chemistry, AU College of Engineering, Visakhapatnam-530003, India

*Corresponding authors: E-mail: lakshmijeevan2000@gmail.com

Received: 27 February 2022;

Accepted: 1 May 2022;

Published online: 18 July 2022;

AJC-20891

Nanostructured zinc stannate binary semiconducting metal nanoparticles are having considerable attention owing to their special and unique properties rendering them suitable for a wide range of variety applications. In the quest to further improve the physico-chemical properties, an interest in ternary complex oxides has become noticeable in recent times. Zinc stannate nanoparticles or zinc tin oxide (ZTO) is a class of ternary oxides, which are known for their stable properties under extreme conditions, higher electron conductivity and mobility compared to its binary counterparts and other interesting optical properties. Among the different methods of synthesizing ZTO nanostructures, the autoclave method is an attractive green technique, which is carried out at low temperatures. In this work, we summarized the conditions leading to the growth of ZTO nanostructures using the hydrothermal method, evaluated few of its antimicrobial applications and compared with reported literature.

Keywords: Hydrothermal method, Zinc stannate nanoparticles.

INTRODUCTION

Zinc stannate (ZnSnO₃ or Zn₂SnO₄) is known to act as ternary semiconducting material [1] and pertaining to the property, it is able to exhibit high electron mobility, electrical conductivity and widely used in piezoelectric nanodevices, photovoltaic devices, polymer-based electronics, etc. [2-5]. They belong to perovskite group of oxides and generally crystallized in ilmenite structure enabled with face-centered-cubic (fcc) closed packing [6]. Various synthesis routes such as thermal evaporation [7], co-precipitation [8], low temperature ion-exchange [9], solvothermal [10], high-temperature calcination [11], sol-gel [12] and hydrothermal methods [13-16] were incorporated to form these materials with high purity.

Wang *et al.* [17] demonstrated the synthesis of zinc stannate nanoparticles (ZTO NPs) in which the morphology was observed to be nanosheets embedded with hollow spheres. Hydrothermal method was used by the research group, by including cetyltrimethylammonium bromide (CTAB) as the mineraliser. Miyauchi *et al.* [18] have performed the synthesis of polyhedral ZTO microcrystals by wet chemical methods at 85 °C. Zeng *et al.* [19] reported the formation of ZTO nanocages,

through zinc acetate and tin(IV) chloride as the precursors via hydrothermal method. The method was successful in forming the nanoparticles in the range of 200-400 nm scale, which were used in the gas-sensing properties. Huang *et al.* [20] prepared porous ZTO nanocubes through zinc sulphate and tin(IV) chloride as the precursors through thermal treatment method. The nanoparticles obtained in this methodology was observed to be pH sensitive and the particles were formed in the range of 80-100 nm at pH 12.0 and 280-310 nm near pH 12.6. The nanoparticles were used in the gas-sensing applications and photocatalytic degradation of rhodamine B solution (50 mL of 10 mg L⁻¹). Wang *et al.* [21] reported the antibacterial efficiency of ZTO (Zn₂SnO₄) nanoparticles, which were synthesized through hydrothermal method with chloride salts of zinc and tin as the precursors.

Over the past years, the microbial contamination has been identified to be increasing on par with the growing advancements in the scientific research [21]. Contamination by microorganisms is of great concern in a variety of areas, such as medical devices, healthcare products, water purification systems, hospitals, dental, office equipment, food packaging, food storage and household sanitation [22,23]. In order to inhibit their

growth, various materials have been used. Some of these materials are metal oxide nanoparticles like TiO₂, ZnO, Fe₂O₃, WO₃, etc. [24,25]. Nano-metal composites are other biocompatible materials, which are efficient in restricting the growth of the microorganisms. Composites of TiO₂ such as *x%* graphene-oxide-TiO₂ were reported to display efficient antibacterial and antifungal activities [25]. The materials were able to control the growth of various microorganisms like *Escherichia coli*, *Staphylococcus aureus*, *Salmonella paratyphi*, *Bacillus subtilis* [26,27].

It has been observed that there is a significant scope of developing biologically active ZTO nanoparticles in a novel approach, to obtain nanoparticles of different morphology. Therefore, the major objective of the present work is to form ZTO nanoparticles through biosynthetic approach by embedding with leaf extracts of *Aloe barbadensis* mill and *Terminalia catappa*. Pure ZTO nanoparticles (without leaf extract) were also synthesized through hydrothermal method and all the synthesized nanoparticles were characterized using XRD, SEM-EDS and UV-visible spectroscopic techniques. The antimicrobial activity of the synthesized nanoparticles was evaluated against selected bacterial (*Bacillus subtilis*, *S. aureus*, *E. coli* and *P. aeruginosa*) and fungal strains (*A. niger* and *C. albicans*).

EXPERIMENTAL

Zinc stannate nanoparticles (ZTO NPs) were synthesized using stannous chloride (SnCl₂), zinc chloride and sodium hydroxide, which were procured from Qualigens (AR grade) and used without any further purification. The entire process was carried out with double distilled water.

In present work, the ZnSnO₃ nanoparticles were synthesized using hydrothermal method [28] and the antibacterial activity of the nanoparticles was evaluated using agar-well diffusion method [29].

Antimicrobial activity: In order to investigate the antimicrobial activity of the synthesized nanoparticles, microorganisms such as Gram-positive bacteria (*Bacillus subtilis* and *Staphylococcus aureus*), Gram-negative bacteria (*Pseudomonas aeruginosa* and *Escherichia coli*) and fungal strains such as *Aspergillus niger* and *Candida albicans*.

The standardized cultures of test bacteria were first evenly spread onto the surface of Mueller-Hinton agar plates using sterile cotton swabs and fungi was spread on Sabouraud's Dextrose Agar plated using sterile cotton swabs. Five wells (6 mm diameter) were made in each plate with sterile cork borer. Fifty microliters of each of the compound and positive control was added in wells. Streptomycin (100 µg mL⁻¹) was used as the standard drug for comparing the results obtained with the ZTO nanoparticles. Diffusion of compounds, antibiotics and DMSO were allowed at room temperature for 1 h. All the plates were then covered with lids and incubated at 37 °C for 24 h. After incubation, plates were observed for zone of bacterial growth inhibition. The size of inhibition zones was measured and antimicrobial activity of the compounds was expressed in terms of the average diameter of inhibition zone in millimeters. Those compounds, which were unable to exhibit inhibition zone (inhibition zone diameter less than 6 mm) were considered

non-active. Each of the prepared ZTO nanoparticles was tested in triplicate with two independent experiments and mean values of zone of inhibition (ZOI) diameters were determined.

Synthesis of zinc stannate nanoparticles (ZTO NPs)

Biosynthesis: The precursor solution was prepared with 1:1 mole concentrations of zinc chloride and tin chloride. In two separate containers, the above solution was added with the leaf extracts of *Aloe barbadensis* mill and *Terminalia catappa*, which acts as mineralizer. These containers were kept under magnetic stirring for about 3 h, to obtain a perfect blending between the leaf extracts and the chemical precursors. The obtained thick solution was then slowly transferred into a Teflon container, equipped in a stainless-steel autoclave. The autoclave is maintained near 200 °C for 24 h. The obtained powders were then cleaned and annealed at 600 °C for 4 h. Thus, the obtained materials were grinded into fine powders and named as ZTO 11A (leaf extract: *Aloe barbadensis* mill) and 11B (leaf extract: *Terminaliacatappa*), respectively.

Chemosynthesis: Similar procedure was followed for the chemosynthesis of ZTO nanoparticles, in which NaOH solution was used as the mineralizer and it was also able to maintain the pH of the reaction medium. The finally obtained powder was named as ZTO 1:1C.

Biological evolution: In present work, Mueller-Hinton agar medium was used for regular susceptibility testing of bacteria, due to its acceptable reproducibility and satisfactory growth of most pathogens [30]. Sabouraud's dextrose agar was used for susceptibility testing of fungi [31]. These two media were prepared by dissolving synthetic powder in distilled water. The medium was adjusted to pH 7.0 with NaOH (1 N) and made up to 1 L with remaining distilled water. The conical flask was sealed properly with the help of cotton plug. The medium and Petri plates (100 mm × 15 mm) were autoclaved at 121 °C, 15 lbs for 20 min. The autoclaved medium was allowed to cool to 45 °C and transferred into Petri plates (20 mL/plate) under disinfected conditions of laminar airflow.

Characterization: The resulting ZTO nanoparticles were characterized using X-ray diffractometer (PANalytical-X'Pert PRO, Japan) at room temperature using nickel filter CuK α radiation ($\lambda = 1.54059 \text{ \AA}$) over wide range of $10^\circ \leq 2\theta \leq 80^\circ$ with a scanning speed of 2 min⁻¹. UV-vis spectra were recorded using single monochromator UV-2600 (optional ISR-2600Plus, λ up to 1400 nm). The morphology of the as-synthesized samples was investigated by field emission scanning electron microscopy (FESEM, LEO1550).

RESULTS AND DISCUSSION

Powder XRD studies: The crystalline structures of the prepared zinc stannate nanoparticles (ZTO 11A, 11B and 11C) were identified through the PXRD patterns and the same are presented in Fig. 1a-c, respectively. The diffraction planes (104), (110), (105) and (006) were obtained at 2θ 32.1°, 34.4°, 36.5° and 38.6°, respectively, corresponding to the standard ZnSnO₃ material with JCPDS File No. 11-0274 [32]. The average crystallite size (D, nm) was calculated through FWHM method using Debye-Scherrer's equation:

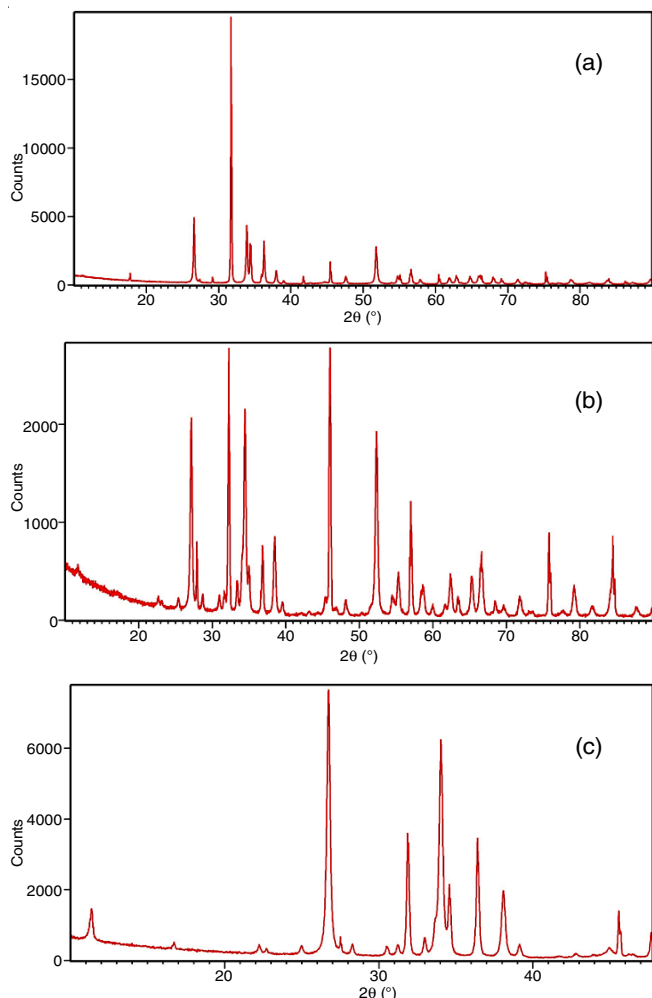


Fig. 1. PXRD spectra of ZTO NPs extracted with (a) *Aloe barbadensis mill*, (b) *Terminalia catappa*, (c) formed through chemo-synthesis

$$D = \frac{K\lambda}{\beta \cos \theta}$$

where, λ is the wavelength of X-ray source used ($\lambda = 1.54 \text{ \AA}$), β is the line width at the half of maximum intensity, k is Scherer constant and θ is denoted Bragg's angle. From this equation, the average crystallite size was obtained as 14.7, 15.1 and 17.9 nm for ZTO 11A, 11B and 11C nanoparticles, respectively.

Morphological studies: The SEM images of all the ZTO NPs are shown in Fig. 2a-c, respectively. It can be observed that the ZTO nanoparticles formed through chemosynthesis method was formed in the form of nano-sheets (Fig. 2c). On including the leaf extracts in the synthesis method, the morphology of the ZTO nanoparticles was modified into formation of agglomerated spherical shaped nanoparticles (Fig. 2a and 2b). In EDS spectra, the presence of the respective atoms (Zn, Sn and O) were clearly observed (Fig. 2d and 2e), which confirms the formation of the ZTO nanoparticles.

UV-Vis studies: The percentage transmittance (% T) of the synthesized ZTO nanoparticles was measured using UV-vis spectrophotometer, over the wavelength range of 350-1000 nm. The %T of ZTO 11A nanoparticles was maximum at 422.7 nm (96.1%) and it has gradually decreased to 94.8% at the maximum wavelength (989 nm) (Fig. 3a). In the similar manner, the %T of ZTO 11B & 11C nanoparticles was highest at 877.1 nm (98.3%) and 969.6 nm (97.07%), respectively (Fig. 3b-c). From these results, it was clearly observed that the % transmittance has increased in the ZTO nanoparticles synthesized with the leaf extract of *Terminalia catappa*. The %transmittance of ZTO 11A nanoparticles, synthesized with the leaf extract of *Aloe barbadensis mill*, was nearer to that of the ZTO 11C nanoparticles. However, at highest wavelength, the difference in the % T of ZTO 11A nanoparticles (998 nm,

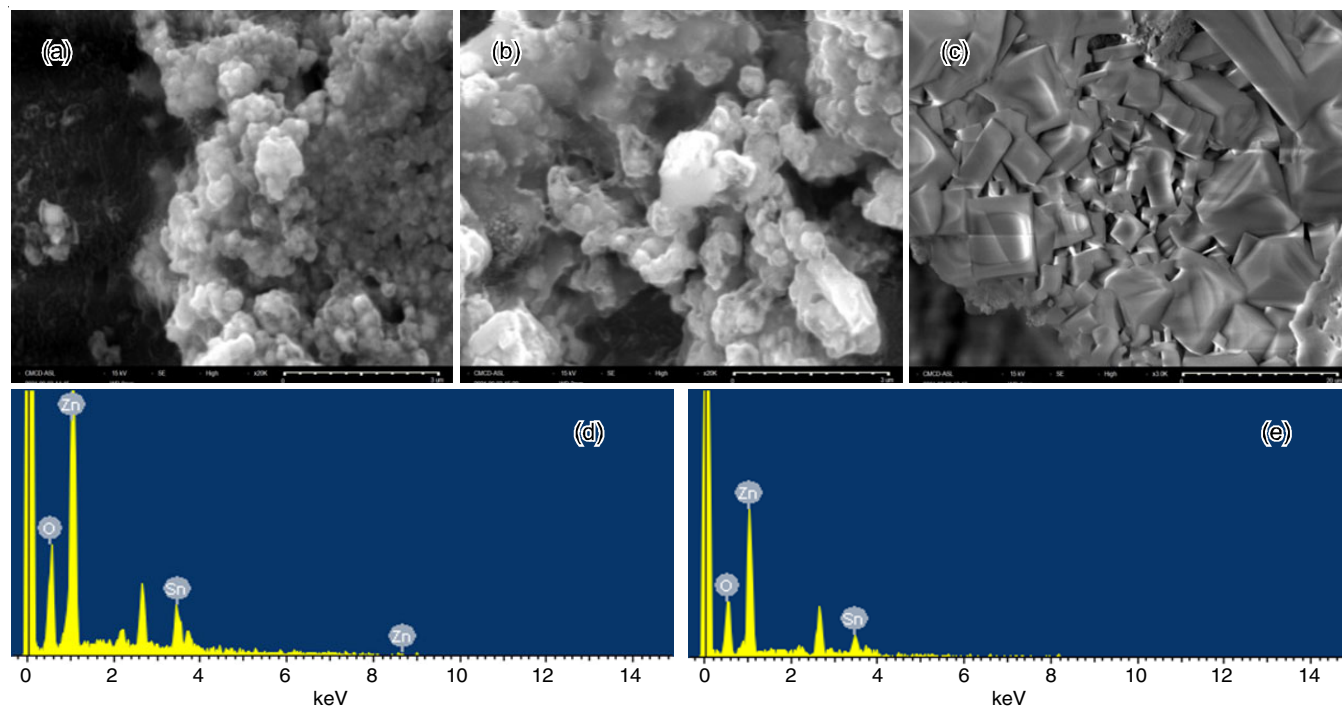


Fig. 2. SEM images of (a) ZTO 11A NPs; (b) ZTO 11B NPs; (c) ZTO 11c NPs; EDS spectra of (d) ZTO 11A NPs; (e) ZTO 11B NPs

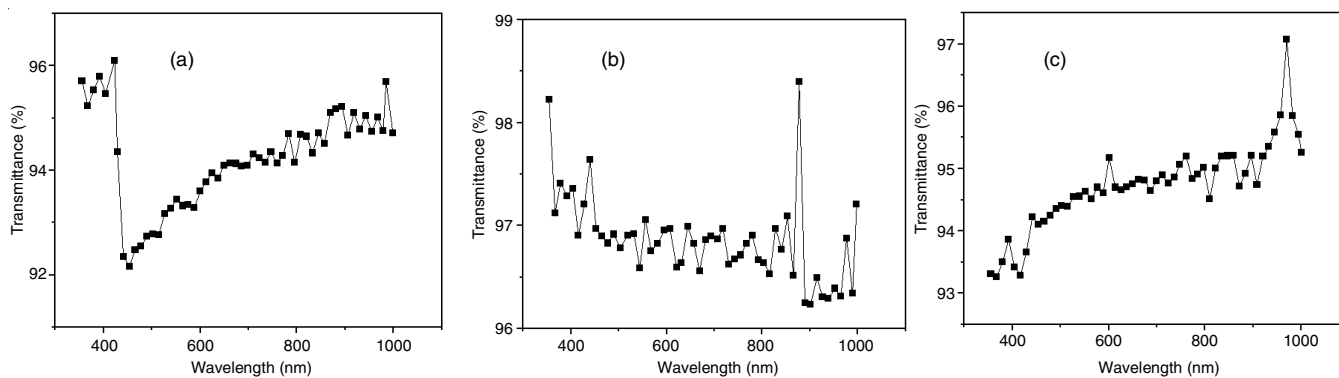


Fig. 3. UV-Vis spectra of ZTO NPs (a) 11A; (at 422.7 nm, T = 96.1%), (b) 11B; (at 877.1 nm, T = 98.3%), (c) 11C; (at 969.6 nm, T = 97.07%)

TABLE-1
ANTIMICROBIAL ACTIVITY OF COMPOUNDS

ZTO NP	Zone of inhibition (mm)											
	Antibacterial activity						Antifungal activity					
	<i>Bacillus subtilis</i>		<i>S. aureus</i>		<i>E. coli</i>		<i>P. aeruginosa</i>		<i>A. niger</i>		<i>C. albicans</i>	
	10 mg	5 mg	10 mg	5 mg	10 mg	5 mg	10 mg	5 mg	10 mg	5 mg	10 mg	5 mg
11A	14	12	12	10	11	10	14	11	7	0	15	11
11B	12	10	10	8	11	9	12	8	8	0	13	9
11C	12	0	10	7	12	9	12	8	8	0	8	0

94.7%) and ZTO 11C nanoparticles (1000 nm, 95.2%) was almost less. Hence, there is a subsequent constructive change in the %T of ZTO nanoparticles on including the leaf extracts.

Antimicrobial studies: The ZOI for all the selected bacterial strains was observed to similar with the prepared ZTO 11B & 11C nanoparticles, at the concentration of 10 mg L⁻¹. However, the ZTO 11A nanoparticles have shown the highest antibacterial activity against all the bacterial strains. Further, the antibacterial activity against *E. coli* was observed to be similar with all the ZTO nanoparticles (Table-1).

In the antifungal activity studies, the ZOI with the fungal strain *A. niger*, has shown almost equal performance with the all the synthesized ZTO nanoparticles. However, growth of the fungal strain *C. albicans* was highly inhibited with the ZTO 11A nanoparticles and the scenario has decreased in the sequential order of ZTO 11B and 11C nanoparticles (Table-1).

The antimicrobial activity studies of zinc stannate nanoparticles synthesized through the leaf extracts of *Aloe barbadensis mill* and *Terminalia catappa*.

In the present studies, all the synthesized zinc stannate nanoparticles (11A & 11B) exhibited the antibacterial and antifungal activities. The nanoparticles formed through biosynthesis method have shown competitive biological activity, on comparison with those formed through chemosynthesis method. This phenomenon was clearly observed in the zone of inhibitions of the bacterial strains *Bacillus subtilis*, *S. aureus*, *P. aeruginosa* and the fungal strain *C. albicans*.

Conclusion

Zinc stannate nanoparticles with composition ZnSnO₃ (ZTO) were synthesized by using reducing/stabilizing agents such as the leaf extracts of *Aloe barbadensis mill* and *Terminalia catappa*. Chemical synthesis was also conducted with NaOH as the mineralizer. The XRD plots have revealed the formation

of corresponding diffraction planes of the ZTO nanoparticles and the average crystallite size of the nanoparticles was observed to form in the range of 14-18 nm. On forming the nanoparticles through these leaf extracts, the morphology has change from nanoplates to nanospherical shaped particles. Further, the transmittance of the prepared ZTO nanoparticles formed through biosynthesis was slightly higher than those formed through chemosynthesis. Moreover, the ZTO nanoparticles extracted with *Terminalia catappa* have presented higher biological activity. Further, the ZTO nanoparticles extracted with *Aloe barbadensis mill* have displayed reasonable activity when compared to those synthesized through pure chemical pathway.

ACKNOWLEDGEMENTS

The authors are thankful to the Inorganic Chemistry Laboratory, Andhra University, Visakhapatnam, India for providing the synthesis facilities and nanotechnology lab, AU College of Engineering (A) for providing the characterization analysis.

CONFLICT OF INTEREST

The authors declare that there is no conflict of interests regarding the publication of this article.

REFERENCES

- S. An, Ch. Jin, H. Kim, S. Lee, B. Jeong and Ch. Lee, *NANO: Brief Reports and Reviews*, **7**, 1250013 (2012); <https://doi.org/10.1142/S1793292012500130>
- I. Stambolova, K. Konstantinov, D. Kovacheva, P. Peshev and T. Donchev, *J. Solid State Chem.*, **128**, 305 (1997); <https://doi.org/10.1006/jssc.1996.7174>
- N. Nikolic, T. Sreckovic and M.M. Ristic, *J. Eur. Ceram. Soc.*, **21**, 2071 (2001); [https://doi.org/10.1016/S0955-2219\(01\)00174-1](https://doi.org/10.1016/S0955-2219(01)00174-1)

4. T.J. Coutts, D.L. Young, X. Li, W.P. Mulligan and X. Wu, *J. Vac. Sci. Technol.*, **18**, 2646 (2000); <https://doi.org/10.1116/1.1290371>
5. J. Jie, G. Wang, X. Han, J. Fang, Q. Yu, Y. Liao, B. Xu, Q. Wang and J.G. Hou, *J. Phys. Chem. B*, **108**, 8249 (2004); <https://doi.org/10.1021/jp049230g>
6. B. Geng, C. Fang, F. Zhan and N. Yu, *Small*, **4**, 1337 (2008); <https://doi.org/10.1002/sml.200701177>
7. J.Q. Xu, X.H. Jia, X.D. Lou, G.X. Xi, J.J. Han and Q.H. Gao, *Sens. Actuators B Chem.*, **120**, 694 (2007); <https://doi.org/10.1016/j.snb.2006.03.033>
8. P. Prabhakaran, M.V.A. Raj, J.J. Mathen, S. Pratap and J. Madhavan Eds.: J. Ebenezer, Hollow ZnSnO₃ Crystallites: Structural, Electrical and Optical Properties, In: Recent Trends in Materials Science and Applications. Springer Proceedings in Physics, Springer, Cham., vol. 189 (2017).
9. X.Y. Xue, Y.J. Chen, Y.G. Liu, S.L. Shi, Y.G. Wang and T.H. Wang, *Appl. Phys. Lett.*, **88**, 201907 (2006); <https://doi.org/10.1063/1.2203941>
10. G. Sun, S. Zhang and Y. Li, *Int. J. Photoenergy*, **2014**, 580615 (2014); <https://doi.org/10.1155/2014/580615>
11. J.B. Shi, P.F. Wu, H.S. Lin, Y.T. Lin, H.W. Lee, C.T. Kao, W.H. Liao and S.L. Young, *Nanoscale Res. Lett.*, **9**, 210 (2014); <https://doi.org/10.1186/1556-276X-9-210>
12. Y. Zhao, L. Hu, H. Liu, M. Liao, X. Fang and L. Wu, *Sci. Rep.*, **4**, 6847 (2015); <https://doi.org/10.1038/srep06847>
13. X. Lou, X. Jia, J. Xu, S. Liu and Q. Gao, *Mater. Sci. Eng. A*, **432**, 221 (2006); <https://doi.org/10.1016/j.msea.2006.06.010>
14. E.L. Foletto, J.M. Simões, M.A. Mazutti, S.L. Jahn, E.I. Muller, L.S.F. Pereira and E.M.M. Flores, *Ceram. Int.*, **39**, 4569 (2013); <https://doi.org/10.1016/j.ceramint.2012.11.053>
15. Y.X. Gan, A.H. Jayatissa, Z. Yu, X. Chen and M. Li, *J. Nanomater.*, **2020**, 8917013 (2020); <https://doi.org/10.1155/2020/8917013>
16. V. Šepelák, S.M. Becker, I. Bergmann, S. Indris, M. Scheuermann, A. Feldhoff, C. Kübel, M. Bruns, N. Stürzl, A.S. Ulrich, M. Ghafari, H. Hahn, C.P. Grey, K.D. Becker and P. Heitjans, *J. Mater. Chem.*, **22**, 3117 (2012); <https://doi.org/10.1039/c2jm15427g>
17. W.W. Wang, Y.J. Zhu and L.X. Yang, *Adv. Funct. Mater.*, **17**, 59 (2007); <https://doi.org/10.1002/adfm.200600431>
18. M. Miyauchi, Z. Liu, Z.-G. Zhao, S. Anandan and K. Hara, *Chem. Commun.*, **46**, 1529 (2010); <https://doi.org/10.1039/b921010e>
19. Y. Zeng, T. Zhang, H. Fan, W. Fu, G. Lu, Y. Sui and H. Yang, *J. Phys. Chem. C*, **113**, 19000 (2009); <https://doi.org/10.1021/jp905230h>
20. J. Huang, X. Xu, C. Gu, W. Wang, B. Geng, Y. Sun and J. Liu, *Sens. Actuators B Chem.*, **171-172**, 572 (2012); <https://doi.org/10.1016/j.snb.2012.05.036>
21. F. Wang, Z. Shi, F. Gong, J.T. Jiu and M. Adachi, *Chin. J. Chem. Eng.*, **15**, 754 (2007); [https://doi.org/10.1016/S1004-9541\(07\)60158-X](https://doi.org/10.1016/S1004-9541(07)60158-X)
22. Y.S. Zhou and W.G. Jiang, *Chin. J. Chem. Eng.*, **10**, 349 (2002).
23. Q.C. Ling, J.Z. Sun and Q.Y. Zhou, *Appl. Surf. Sci.*, **254**, 3236 (2008); <https://doi.org/10.1016/j.apsusc.2007.11.001>
24. S.-H. Choi, D. Hwang, D.-Y. Kim, Y. Kervella, P. Maldivi, S.-Y. Jang, R. Demadrille and I.-D. Kim, *Adv. Funct. Mater.*, **23**, 3146 (2013); <https://doi.org/10.1002/adfm.201203278>
25. R. Somasekhar and D.S. Paul, *Res. J. Chem. Environ.*, **10**, 80 (2021); <https://doi.org/10.25303/2510rjce8083>
26. B. Koneru, Y. Shi, Y.-C. Wang, S. Chavala, M. Miller, B. Holbert, M. Conson, A. Ni and A. Di Pasqua, *Molecules*, **20**, 19690 (2015); <https://doi.org/10.3390/molecules201119650>
27. Z. Chen, M. Cao and C. Hu, *J. Phys. Chem. C*, **115**, 5522 (2011); <https://doi.org/10.1021/jp111785t>
28. P.M. Aneesh, K.A. Vanaja and M.K. Jayaraj, *Nanophoton. Mater.* **IV**, **6639**, 66390J (2007); <https://doi.org/10.1117/12.730364>
29. P.K. Stoimenov, R.L. Klinger, G.L. Marchin and K.J. Klabunde, *Langmuir*, **18**, 6679 (2002); <https://doi.org/10.1021/la0202374>
30. C. Fernández-Mazarrasa, O. Mazarrasa, J. Calvo, A. del Arco and L. Martínez-Martínez, *J. Clin. Microbiol.*, **47**, 827 (2009); <https://doi.org/10.1128/JCM.02464-08>
31. O. Akgul and N. Cerikcioglu, *Mycopathologia*, **167**, 357 (2009).
32. B. Ayesha, U. Jabeen, A. Naeem, P. Kasi, M.N.K. Malghani, S.U. Khan, J. Akhtar and M. Aamir, *Results Chem.*, **2**, 100023 (2020); <https://doi.org/10.1016/j.rechem.2020.100023>